Tensor Force Manifestations in *Ab Initio* Study of the ^{2}H(d,γ)^{4}He, ^{2}H(d,p)^{3}H, and ^{2}H(d,n)^{3}He Reactions

K. Arai,[1,*] S. Aoyama,[2] Y. Suzuki,[3,4] P. Descouvemont,[5] and D. Baye[6,5]

[1]*Division of General Education, Nagaoka National College of Technology, 888 Nishikatakai, Nagaoka, Niigata 940-8532, Japan*
[2]*Center for Academic Information Service, Niigata University, Niigata 950-2181, Japan*
[3]*Physics Department, Niigata University, Niigata 950-2181, Japan*
[4]*RIKEN Nishina Center, Wako 351-0198, Japan*
[5]*Physique Nucléaire Théorique et Physique Mathématique, C.P.229, Université Libre de Bruxelles, B-1050 Brussels, Belgium*
[6]*Physique Quantique, CP165/82, Université Libre de Bruxelles, B-1050 Brussels, Belgium*
(Received 20 June 2011; published 23 September 2011)

The ^{2}H(d,p)^{3}H, ^{2}H(d,n)^{3}He, and ^{2}H(d,γ)^{4}He reactions are studied at low energies in a multichannel *ab initio* model that takes into account the distortions of the nuclei. The internal wave functions of these nuclei are given by the stochastic variational method with the AV8$'$ realistic interaction and a phenomenological three-body force included to reproduce the two-body thresholds. The obtained astrophysical S factors are all in very good agreement with the experiment. The most important channels for both transfer and radiative capture are identified by comparing to calculations with an effective central force. They are all found to dominate thanks to the tensor force.

DOI: 10.1103/PhysRevLett.107.132502 PACS numbers: 25.45.−z, 21.60.De, 26.20.Cd, 27.10.+h

The nonvanishing value of the quadrupole moment of the deuteron [1] is the best direct evidence for the existence of a tensor force [2]. The deformation of the deuteron indicates that nucleon-nucleon (*NN*) forces cannot be purely central but must mix S and D components in wave functions. The confirmation of the existence of a tensor component depending on the direction of the total spin of the two nucleons was a further success of Yukawa's meson theory. Taking correctly the tensor force into account and evaluating its influence are among the main challenges of nuclear physics. The tensor force is known to give an important attractive contribution to the binding energies of nuclei, but this can be seen only through complicated calculations. The role of the tensor force, among others, is stressed in relation to the evolution of nuclear spectra in light nuclei in Ref. [3].

The role of the tensor force is even more difficult to disentangle in reactions. However, the four-body ^{2}H(d,γ)^{4}He reaction offers a direct manifestation of the tensor force because its cross section at low energies is affected by D-wave components in the relevant wave functions and hence is very sensitive to the tensor component in the *NN* interaction [4–7]. Indeed, the energy dependence of its cross section at very low energies can be explained only by the fact that the capture proceeds from an initial s wave, i.e., without a centrifugal barrier. However, such a transition to the 0^+ ^{4}He ground state is not possible without D components. As we shall see, the same manifestation of the tensor force occurs in the reactions ^{2}H(d,p)^{3}H and ^{2}H(d,n)^{3}He, although in a less simple way.

The $d+d$ reactions have been studied at very low energies for astrophysical reasons. Indeed, according to the big bang theory, the primordial deuterons play a key role to synthesize ^{4}He through the reactions ^{2}H(d,p)^{3}H and ^{2}H(d,n)^{3}He, followed by ^{3}H(d,n)^{4}He and ^{3}He(d,p)^{4}He. The reaction ^{2}H(d,γ)^{4}He might also have an effect on the abundances of primordial elements. The knowledge of the reaction cross sections at the energies of astrophysical relevance is of great interest not only for establishing imprints of the properties of nuclei in the Universe but also for a detailed understanding of the interplay between the structure and reactions of these nuclei.

Because of the complexity of the *NN* interaction, *ab initio* studies on scattering and reactions have first been limited mostly to three-nucleon systems [8]. It is only recently that several approaches, e.g., Green's function Monte Carlo method [9], the no-core shell model [10], and continuum discretization [11] were applied to scattering calculations. Closely related to the present study are coupled-channels calculations including $n+h$, $p+t$, and $d+d$, where t and h stand for ^{3}H and ^{3}He, respectively [12,13].

In this Letter, we present *ab initio* cross section calculations for the radiative capture process, ^{2}H(d,γ)^{4}He, and the transfer reactions ^{2}H(d,p)^{3}H and ^{2}H(d,n)^{3}He. These precise four-nucleon microscopic calculations of the three reactions simultaneously allow us to emphasize the influence of the tensor force not only on the capture reaction [4–7] but also on the two transfer reactions.

We have recently applied a multichannel microscopic cluster model to study the phase shifts of the $p+h$ [14], $d+d$, $p+t$, and $n+h$ [15] scatterings. This model combines the stochastic variational method [16,17] with the microscopic R-matrix method (MRM) [18]. Here we use wave functions that are obtained by a combination of

Gaussian-type functions by solving Schrödinger equations for the intrinsic Hamiltonians. The relative motion functions between the nuclei are also expanded in terms of Gaussian bases. Matrix elements needed to solve continuum problems are reduced to exactly the same as those in bound-state problems, and they can be analytically obtained [15]. One of the advantages of this formulation is that the inclusion of excited or pseudostates of the nuclei is quite easy. When two nuclei approach each other, one or both of them can be distorted because realistic NN interactions can affect considerably both space and spin parts of their wave functions, so that it is crucially important to take account of distorted configurations.

The Hamiltonian we use reads

$$H = \sum_{i=1}^{4} T_i - T_{\rm cm} + \sum_{i<j}^{4} V_{ij} + \sum_{i<j<k}^{4} V_{ijk}, \qquad (1)$$

where T_i is the nucleon kinetic energy, $T_{\rm cm}$ is the kinetic energy of the center of mass, and V_{ij} and V_{ijk} are two-body and three-body interactions, respectively. The Coulomb potential between protons is included. The p-n mass difference is ignored. For V_{ij} we use two different realistic potentials, AV8$'$ [19] and G3RS [20], that consist of central, tensor, and spin-orbit pieces. Table I lists some properties of the relevant nuclei obtained with these potentials. The number N of basis functions used to construct the cluster wave function had to be chosen rather small to make the cross section calculation possible within reasonable computer times. Because we optimized the basis functions by using the stochastic variational method, the properties listed in Table I are pretty close to those of more extensive calculations [21] despite the use of smaller N values. The G3RS potential is softer than the AV8$'$ potential and gives slightly smaller D-state probabilities for d, t, h, and α [21]. It is crucial to reproduce the two-body thresholds of $d+d$, $t+p$, and $h+n$ for comparing calculated astrophysical S factors to the experiment. Thus we include a phenomenological three-body force taken from Ref. [22]. Because our main aim is to clarify the role of the tensor force, it is useful to compare results obtained with the realistic interactions with that of an effective NN interaction that contains no tensor force. We adopt the Minnesota (MN) central potential [23] with $u = 1.0$. No three-body force is necessary with the MN potential.

TABLE I. Ground-state energies E and D-state probabilities P_D obtained with the AV8$'$ and G3RS potentials and a three-body force. N is the number of basis functions.

		AV8$'$		G3RS		Exp.
Nucleus	N	E	P_D	E	P_D	E
d	8	-2.18	5.9	-2.13	5.0	-2.22
t	30	-8.22	8.4	-8.24	6.9	-8.48
h	30	-7.55	8.3	-7.58	6.9	-7.72
α	2370	-27.99	13.8	-28.23	11.2	-28.30

The total wave function with the angular momentum JM and parity π is given in terms of a combination of various channel components $\Psi_c^{\rm JM\pi}$:

$$\Psi_c^{\rm JM\pi} = \mathcal{A}[[\Phi^a_{I_a\pi_a}\Phi^b_{I_b\pi_b}]_I \chi_c^J]_{\rm JM}, \qquad (2)$$

where $\Phi^a_{I_a\pi_a}$ and $\Phi^b_{I_b\pi_b}$ are, respectively, antisymmetrized intrinsic wave functions of nuclei a and b that compose channel c, χ_c^J is the relative motion function with the orbital momentum ℓ, and $\mathcal{A}$ is an antisymmetrizer acting between the clusters. The square brackets $[I_aI_b]_I$ denote the angular momentum coupling. All possible I, ℓ sets with $\ell \le 2$ are included. The channels included in the calculation are $t(1/2^+) + p$, $h(1/2^+) + n$, and $d(1^+) + d(1^+)$, where, for example, t stands for a triton not only in its ground state but also in its excited pseudostates with $\frac{1}{2}^+$. These pseudostates are obtained together with the ground state by diagonalizing the Hamiltonian for the $n+n+p$ system. The pseudostates of h and d are included as well. We also include other two-body channels $np(0^+) + np(0^+)$ and $2n(0^+) + 2p(0^+)$. Here each two-nucleon system is unbound but included to take into account possible distortions of the incoming d's. Their wave functions are obtained by the same S-wave basis function used in the d cluster and are approximated by a bound-state type of wave function.

The relative motion functions χ_c^J in Eq. (2) are determined with the MRM, in which the configuration space is divided into two regions, internal and external, by a channel radius. The relative motion function $\chi^J_{cm_\ell}(\boldsymbol{r})$ in the inner region is expanded in terms of Gaussian basis functions as $\sum_i C_i r^\ell \exp(-\lambda_i r^2) Y_{\ell m_\ell}(\hat{\boldsymbol{r}})$ with a suitable set of λ_i's. With the help of the Bloch operator it is smoothly connected, at the channel radius, to the asymptotic form of the relative wave function that contains the scattering S-matrix to be determined. We choose a suitable number of bases $\{\lambda_i\}$ so as to make the S matrix stable and independent of the channel radius. A detailed analysis of the phase shifts obtained in the MRM is reported elsewhere [15]. The cross sections for the radiative capture and transfer reactions are calculated as in Ref. [24]. The α properties with the full multichannel MRM basis are given in Table I.

First we discuss the radiative capture reaction ^{2}H$(d,\gamma)^4$He. The symmetry of the two d's imposes the condition $I+\ell$ even, which together with the addition of the angular momenta $\boldsymbol{I} + \boldsymbol{\ell} = \boldsymbol{J}$ and the parity $\pi = (-1)^\ell \pi_a\pi_b$ leads to the following relationship between the multipole ($EM\lambda$) of electromagnetic transition and the incoming dd channel $(^{(2I+1)}\ell_J)$: $^3P_1$ for $E1$, $^5D_1$ for $M1$, $^5S_2$, $^1D_2$, and $^5D_2$ for $E2$, etc. Because of isospin conservation, one expects the radiative capture to proceed predominantly via the $E2$ transition at low energies. With the present Hamiltonian, the forbidden $E1$ transition represents less than 15% at its maximum near 200 keV but decreases at lower energies because of an initial p wave and gives a minor contribution to $S(0)$. Notice that the larger percentage in Ref. [7] seems to be due to a smaller $E2$ component. We thus discuss the cross section assuming $E2$ transitions. Table I indicates that the $L_i = 2$ component of the incoming dd state in the s wave is 10%–11% and the $L_f = 2$ component of the final α state is 11%–14%, where L stands for the total orbital angular momentum of the system. We expect the $E2$ transition to mainly occur in three paths: (i) $L_i = 2(\ell = 0)$, $L_f = 0$, (ii) $L_i = 0(\ell = 0)$, $L_f = 2$, and (iii) $L_i = 2(\ell = 2)$, $L_f = 0$. The first two paths occur in the incoming ${}^5S_2$ channel and are favored by the absence of a centrifugal barrier. They depend on the admixture of D-state probabilities in the dd (i) and α (ii) wave functions. Hence they are possible only when the NN interaction contains a tensor component. Paths (i) and (iii) are favored by the large $L_f = 0$ final component in ^{4}He.

Figure 1 displays the calculated astrophysical S factor for the ${}^2\mathrm{H}(d,\gamma){}^4\mathrm{He}$ reaction. Results with both AV8′ (solid line) and G3RS (dashed line) potentials very well reproduce the experimental data, especially their flat behavior at low energies, whereas the MN potential (dotted curve) shows a rapidly decreasing pattern as E_{cm} decreases, typical of an initial d wave. The extrapolated $S(0)$ value is 6.3×10^{-3} (AV8′) and 8.1×10^{-3} eV b (G3RS). To clarify the energy dependence of the S factor, we show in Fig. 2 the contributions of the three incoming dd channels to the S factor: ${}^5S_2$ (dotted line), ${}^1D_2$ (dashed line), and ${}^5D_2$ (dash-dotted line). The first two channels give equal contributions at about 0.3 MeV. Below that energy, the ${}^5S_2$ channel overwhelms the ${}^1D_2$ channel, yielding the flat behavior, whereas above that energy the ${}^1D_2$ channel contributes more than the ${}^5S_2$ channel. The contribution of the ${}^5D_2$ channel is negligible below 10 MeV. The $E2$ transition in the case of the MN potential occurs through path (iii), and the corresponding S factor (dotted curve in Fig. 1) is quite similar to the ${}^1D_2$ contribution (dashed line in Fig. 2). The energy dependence of the S factor, manifestly different between the realistic and effective interactions, is attributed to the role played by the tensor force. Without tensor force, the astrophysical S factor of the ${}^2\mathrm{H}(d,\gamma){}^4\mathrm{He}$ reaction cannot be reproduced below 0.3 MeV. Notice that the low-energy S factors for both potentials are not correlated with the deuteron D-state probabilities of Table I. This is due to the interference between paths (i) and (ii) where both S and D waves contribute.

We now discuss the astrophysical S factors for the reactions, ${}^2\mathrm{H}(d,p){}^3\mathrm{H}$ and ${}^2\mathrm{H}(d,n){}^3\mathrm{He}$. The NN interaction is responsible for these transfer reactions, and no apparent selection on J^π values is possible. We have taken into account the states with $0^\pm$, $1^\pm$, and $2^\pm$. Figure 3 compares the astrophysical S factors between the theory and experiment. The extrapolated $S(0)$ values for ${}^2\mathrm{H}(d,p){}^3\mathrm{H}$ and ${}^2\mathrm{H}(d,n){}^3\mathrm{He}$ reactions are 56 and 54 keV b with the AV8′ potential. The results obtained with the realistic potentials, both AV8′ and G3RS, are in very good agreement with experiment, while the MN potential gives too small cross sections. To clarify the reason for this difference, we analyze the contribution of each J^π state to the S factor. Figure 4(a) exhibits the partial contribution to the ${}^2\mathrm{H}(d,p){}^3\mathrm{H}$ S factor for AV8′. The contribution of the 1^+ state is negligible in this energy region. The 2^+ contribution is largest below 60 keV, and the 0^+ contribution is not that large. This difference is probably due to the fact that the tensor force, which is responsible for the 2^+ contribution as discussed below, has a longer-ranged attraction compared to the central force responsible for the 0^+ contribution. The summed contributions of the negative parity states, in which the 1^- state is dominant, rapidly increase with increasing energy. In Fig. 4(b), we plot the decomposition of the 2^+ contribution according to transfer processes specified by the incoming dd and final tp channels. For 2^+ the tp channel contains ${}^1D_2$ and ${}^3D_2$. Thus the transfer reaction in 2^+ proceeds from the three incoming dd channels to the two outgoing tp channels. Among these, most important three paths are drawn: ${}^5S_2 \rightarrow {}^1D_2$ (dotted line), ${}^5S_2 \rightarrow {}^3D_2$ (dashed line), and ${}^1D_2 \rightarrow {}^1D_2$ (dash-dotted line). The transfer process ${}^5S_2 \rightarrow {}^3D_2$

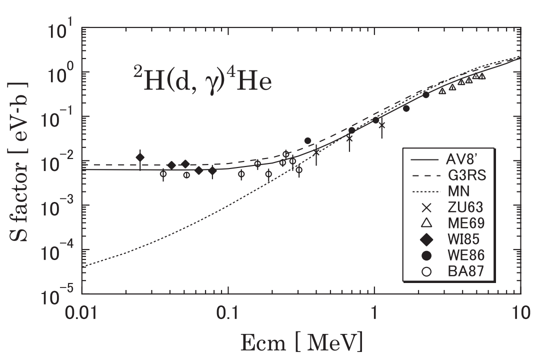

FIG. 1. Astrophysical S factor of the ${}^2\mathrm{H}(d,\gamma){}^4\mathrm{He}$ reaction. Results calculated with the realistic (AV8′ and G3RS) and effective (MN) potentials are compared to the experiment [25].

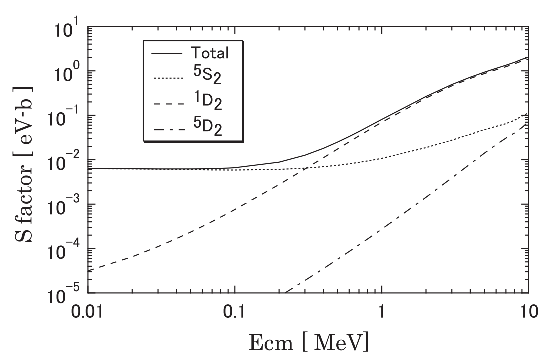

FIG. 2. Contributions of the three incoming dd channels, ${}^5S_2$, ${}^1D_2$, and ${}^5D_2$, to the astrophysical S factor of the ${}^2\mathrm{H}(d,\gamma){}^4\mathrm{He}$ reaction. The AV8′ potential is used.

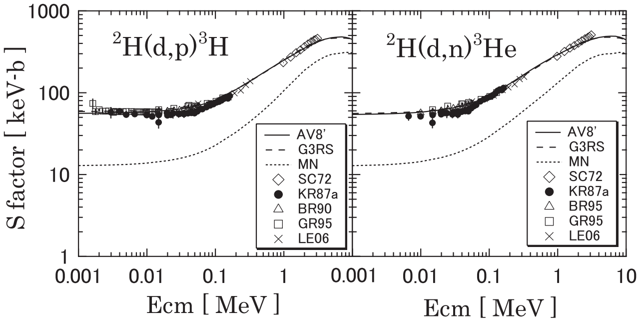

FIG. 3. Astrophysical S factors of the ^{2}H$(d,p)^3$H and ^{2}H$(d,n)^3$He reactions. Results calculated with the realistic (AV8$'$ and G3RS) and effective (MN) potentials are compared to the experiment [25,26].

dominates over the others at low energies. The main component of the dd $^5S_2$ channel consists of $L_i = 0$, $S_i = 2$, while that of the final outgoing channel has $L_f = 2$, $S_f = 1$, where S_i and S_f are the total spins of the initial and final states, respectively. This process is realized by the tensor force but cannot occur with the MN potential. Similarly, the $^5S_2 \rightarrow {}^1D_2$ process is realized by the tensor force, but its contribution becomes smaller than the $^3D_2$ case because of different spin structures. Namely, the four nucleons in $^5S_2$ that initially have $S_i = 2$ with [4] symmetry have stronger tensor couplings with the [31] $S_f = 1$ state in $^3D_2$ than with the [22] $S_f = 0$ state in $^1D_2$. The $^1D_2 \rightarrow {}^1D_2$ process can occur by the central force. Therefore, with the MN potential, the astrophysical S factor is contributed mainly by the 0^+ and negative parity states at low energies and by the $^1D_2 \rightarrow {}^1D_2$ transition at higher energies, but it misses the most important $^5S_2 \rightarrow {}^3D_2$ transition. This is the reason why the MN potential underestimates the S factor. The tensor force again plays a crucial role in reproducing correctly the S factor for the transfer reactions.

In conclusion, the three reactions of astrophysical interest, ^{2}H$(d,\gamma)^4$He, ^{2}H$(d,p)^3$H, and ^{2}H$(d,n)^3$He, are simultaneously studied in an *ab initio* model using realistic NN interactions. The distortion of the nuclei is taken into account. The astrophysical S factors of these reactions are all very well reproduced. The radiative capture occurring via $E2$ is made possible through the D-wave components of ^{2}H and ^{4}He, which is a direct manifestation of the tensor force. A further step will be a precise explanation of the properties of the $E1$ and $M2$ components [7] and of the smallness of $M1$. In that case the use of a more realistic three-nucleon interaction will be desirable as exemplified in Ref. [9]. The transfer reactions near zero energy mainly occur from the transition of the dd $^5S_2$ channel to the D-wave continuum of $t + p$ or $h + n$, which is also due to the tensor force. Without a tensor force the flat behavior of the S factor of these reactions at low energies cannot be reproduced as shown by the failure of calculations with an effective force, and the evolution of the Universe after the primordial nucleosynthesis would be quite different from what we know.

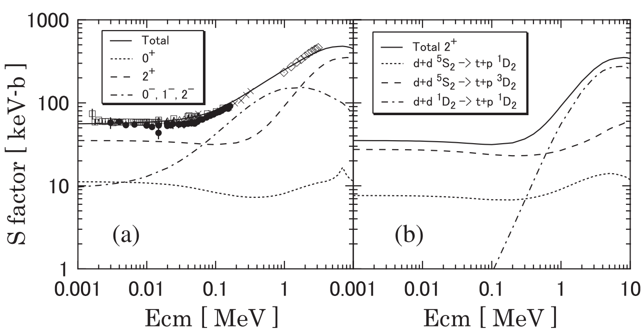

FIG. 4. (a) Contributions of the different J^π states to the astrophysical S factor of the ^{2}H$(d,p)^3$H reaction. (b) Decomposition of the 2^+ contribution according to the incoming dd and outgoing tp channels. The AV8$'$ potential is used.

We thank R. Kamouni for his help in early stages of this work. This work presents research results of the Bilateral Joint Research Project of the JSPS (Japan) and the FNRS (Belgium) and of the IAP program P6/23 of the FSTC (Belgium). Y. S. is supported in part by a Grant-in-Aid for Scientific Research (No. 21540261). We thank T2K-Tsukuba (Super Computer) for partial support.

*arai@nagaoka-ct.ac.jp

[1] J. M. B. Kellogg, I. I. Rabi, N. F. Ramsey, and J. R. Zacharias, Phys. Rev. **55**, 318 (1939).
[2] H. A. Bethe, Phys. Rev. **55**, 1261 (1939).
[3] R. B. Wiringa and S. C. Pieper, Phys. Rev. Lett. **89**, 182501 (2002).
[4] H. J. Assenbaum and K. Langanke, Phys. Rev. C **36**, 17 (1987).
[5] K. Langanke, in *Advances in Nuclear Physics*, edited by J. W. Negele and E. Vogt (Plenum, New York, 1994), Vol. 21, p. 85.
[6] A. Arriaga, V. R. Pandharipande, and R. Schiavilla, Phys. Rev. C **43**, 983 (1991).
[7] K. Sabourov *et al.*, Phys. Rev. C **70**, 064601 (2004).
[8] W. Glöckle, H. Witala, D. Hüber, H. Kamada, and J. Golak, Phys. Rep. **274**, 107 (1996).
[9] K. M. Nollett, S. C. Pieper, R. B. Wiringa, J. Carlson, and G. M. Hale, Phys. Rev. Lett. **99**, 022502 (2007); J. Carlson and R. Schiavilla, Rev. Mod. Phys. **70**, 743 (1998).
[10] S. Quaglioni and P. Navratil, Phys. Rev. Lett. **101**, 092501 (2008).
[11] Y. Suzuki, W. Horiuchi, and K. Arai, Nucl. Phys. **A823**, 1 (2009).
[12] A. Deltuva and A. C. Fonseca, Phys. Rev. C **76**, 021001(R) (2007).
[13] H. M. Hofmann and G. M. Hale, Phys. Rev. C **77**, 044002 (2008).
[14] K. Arai, S. Aoyama, and Y. Suzuki, Phys. Rev. C **81**, 037301 (2010).

[15] S. Aoyama, K. Arai, Y. Suzuki, P. Descouvemont, and D. Baye, arXiv:1106.3391.
[16] V. I. Kukulin and V. M. Krasnopol'sky, J. Phys. G **3**, 795 (1977).
[17] K. Varga, Y. Suzuki, and R. G. Lovas, Nucl. Phys. **A571**, 447 (1994); K. Varga and Y. Suzuki, Phys. Rev. C **52**, 2885 (1995).
[18] D. Baye, P.-H. Heenen, and M. Libert-Heinemann, Nucl. Phys. **A291**, 230 (1977); P. Descouvemont and D. Baye, Rep. Prog. Phys. **73**, 036301 (2010).
[19] B. S. Pudliner, V. R. Pandharipande, J. Carlson, S. C. Pieper, and R. B. Wiringa, Phys. Rev. C **56**, 1720 (1997).
[20] R. Tamagaki, Prog. Theor. Phys. **39**, 91 (1968).
[21] Y. Suzuki, W. Horiuchi, M. Orabi, and K. Arai, Few-Body Syst. **42**, 33 (2008).
[22] E. Hiyama, B. F. Gibson, and M. Kamimura, Phys. Rev. C **70**, 031001 (2004).
[23] D. R. Thompson, M. LeMere, and Y. C. Tang, Nucl. Phys. **A286**, 53 (1977).
[24] K. Arai, D. Baye, and P. Descouvemont, Nucl. Phys. **A699**, 963 (2002).
[25] C. Angulo *et al.*, Nucl. Phys. **A656**, 3 (1999).
[26] D. S. Leonard, H. J. Karwowski, C. R. Brune, B. M. Fisher, and E. J. Ludwig, Phys. Rev. C **73**, 045801 (2006).